This work has been accepted for publication in Applied Spectroscopy.

Access to this work was provided by the University of Maryland, Baltimore County (UMBC) ScholarWorks@UMBC digital repository on the Maryland Shared Open Access (MD-SOAR) platform.

Please provide feedback

Please support the ScholarWorks@UMBC repository by emailing scholarworks-group@umbc.edu and telling us what having access to this work means to you and why it's important to you. Thank you.

Thermally Induced Optical Reflection of Sound (THORS) in Ambient Air: Characterization and Temporal Dynamics

Daniel S. Kazal[1], Alex J. Reardon[1], and Brian M. Cullum[1] [iD]

Abstract

Thermally induced optical reflection of sound (THORS) provides a means to manipulate sound waves without the need for traditional acoustically engineered structures. By photothermally exciting a medium, with infrared light, a barrier can be formed due to abrupt changes in compressibility of the excited medium. Discovery and initial characterization of the THORS phenomenon utilized air saturated with ethanol vapor as the absorbing medium and a CO_2 laser, operating at 9.6 μm, as the excitation source to achieve acoustic reflection efficiencies of 25–30% of the incident wave. In this work, we demonstrate for the first time, the ability to generate THORS barriers in ambient air (i.e., without the need for ethanol vapor). Employing atmospheric water vapor as the absorbing medium and a modulated, multiline carbon monoxide laser, operating at 5.5 ± 0.25 μm, THORS barriers capable of acoustic and ultrasonic reflection–suppression efficiencies greater than 70% are readily generated. To achieve these significant reflection–suppression efficiencies, the temporal dynamics of THORS barriers in ambient air were characterized using 300 kHz ultrasonic pulses incident on the barriers, revealing three different operational regimes. In the first regime, a single laser pulse generates a transient THORS barrier that lasts tens of milliseconds and exhibits minimal acoustic reflectivity. In the second regime, multiple laser pulses interact with the water vapor prior to complete relaxation of the THORS barrier from the previous excitation pulse, resulting in an additive response and reflectivity/suppression efficiencies as great as 72%. Finally, in the third regime, non-modulated continuous wave (CW) excitation of the water vapor occurs resulting in no measurable acoustic reflectivity/suppression from the THORS barrier. This work characterizes these different regimes and the optimal modulation timing to generate efficient continuous acoustic barriers using THORS.

Introduction

The manipulation of sound is critically important to many scientific and engineering fields, including acoustic engineering design, photoacoustic sensing and imaging, acoustic stealth technologies, and secure communications.[1–8] Historically, the manipulation and control of sound waves has been limited by the need for physical structures (e.g., reflectors, dampers, and acoustic channels) where the direction and magnitude of reflected, transmitted, and refracted incident sound waves are controlled through the shape of the physical interface and the differences in compressibility of the dissimilar acoustic transport media.[9–11] Recently, the newly discovered photothermal phenomenon known as thermally induced optical reflection of sound (THORS) has been demonstrated in controlled environments to be capable of providing an alternative means of manipulating sound waves without the need for physical objects for acoustic reflection.[12] By optically exciting a strongly absorbing component in air (e.g., ethanol vapor and water vapor) using infrared laser light, a significant amount of heat can be directly deposited in the air at a specific location(s). As the absorbing

[1]Department of Chemistry, University of Maryland, Baltimore County, Baltimore, MD, USA

Corresponding author:
Brian M. Cullum, Department of Chemistry, University of Maryland, Baltimore County, 1000 Hilltop Circle, Baltimore, MD 21250, USA.
Email: cullum@umbc.edu

chemical species relaxes from its excited vibrational state, the excited molecules collide with the dominant bath gases (N_2, O_2) creating a thermally induced depletion layer along the path of the beam and its immediate surroundings. This localized difference in density of the optically excited air volume compared to the surrounding air that was not excited generates an abrupt change in compressibility in the two volumes at this boundary, resulting in the THORS barrier. The distinct difference in density and compressibility of these two regions results in distinctly different acoustic impedances (z) for each volume, resulting in acoustic reflection. From traditional acoustic theory, when a sound wave is incident on this THORS barrier, the fraction of sound reflected can be determined from Eq. 1, where R is the reflection coefficient, z_1 is the acoustic impedance of the ambient material, and z_2 is the acoustic impedance of the depleted zone

$$R = \sqrt{\frac{(z_1 - z_2)^2}{(z_1 + z_2)^2}} \qquad (1)$$

Discovery and previous demonstration of the THORS phenomenon was restricted to the generation of THORS barriers in a sealed plexiglass chamber containing air saturated with ethanol vapor. Using a CO_2 laser as the excitation source, the laser beam passed into the sealed chamber to excite the ethanol vapor, and created an abrupt change in compressibility of the air in the path of laser beam compared to the immediately surrounding air.[13] This optically generated compressibility barrier was found to be capable of reflecting, and subsequently suppressing transmission of incident audible acoustic waves (between 1–10 kHz) by approximately 25%, as well as allowing sound waves to be optically reflected around corners.[12] To completely suppress the transmission of incident acoustic waves via THORS, it was found that multiple discreet barriers could be generated next to each other with each subsequent barrier further decreasing the amplitude of the incident wave until no measurable transmission was observed.[13] Furthermore, when the CO_2 laser beam was shaped into a ring by optically expanding and masking the center of the beam, an acoustic waveguide (i.e., THORS channel) could be generated, demonstrating significant enhancements in the distance over which sound could be transmitted. In fact, propagation of acoustic waves in these non-idealized channels revealed an acoustic decay of $1/r^{0.6}$ with distance as opposed to the expected $1/r$ decay in normal air in the absence of a channel.[14,15] At this acoustic decay rate, given sufficient laser power, a 70 dB acoustic wave (indoor voice) would theoretically be detectable by the human ear at distances as great as 1 km. Unfortunately, due to the fact that THORS requires a modulated excitation source to generate efficient barriers, and the difference in speed between the propagating acoustic waves and the laser light responsible for generating the barriers, such distances are physically impossible without complicated optical configurations (e.g., alternating concentric

rings of excitation light that do not overlap).[13] However, by understanding the formation and relaxation dynamics of these THORS barriers, it may be possible to create a stable THORS barrier capable of constant acoustic reflection (or waveguiding) employing a modulated excitation source.[16–18]

In this paper, THORS barriers are generated for the first time in ambient air, with water vapor serving as the absorbing species, allowing for the translation of THORS to environments outside of a sealed environmental chamber and potential real-world application. Furthermore, expansion and characterization of the reflectivity of these ambient air-based THORS barriers to ultrasonic frequencies is also performed. Finally, characterization of the temporal dynamics of these air-based THORS barriers is achieved, revealing three distinct operational regimes that allow the reflection–suppression efficiency to be easily manipulated to the desired amount. Among these regimes is one in which highly reflective THORS barriers (greater than 70% reflection–suppression efficiency per barrier) are capable of being generated that exhibit continuous acoustic reflectivity despite being excited with an optically modulated laser.

Experimental

Generation of THORS barriers in ambient air is performed by exciting the vibrational bands of ambient water vapor, between 1900 cm^{-1} and 1300 cm^{-1},[19] using a high-powered carbon monoxide (CO) laser (Coherent Inc., Diamond J-3-5 Series) emitting 5.50 ± 0.25 μm light. The beam waist diameter of the CO laser is 4 ± 1 mm at $1/e^2$. No optics external to the laser aperture were employed in these studies. Following absorption, an abrupt difference in compressibility of the excited air (relative to the surrounding air) occurs, due to thermal relaxation of the excited water molecules and subsequent molecular depopulation of the water and the other bath gases they collide with within the excited volume. The maximum output power of the CO laser, 250 W, is capable of being electronically attenuated by reducing the overall applied RF energy of the laser using a 1 MHz intra-pulse modulation, with the duty cycle of the intra-pulse modulation being directly related to the output power. Modulation of the resulting variable power laser beam to the desired output frequency and duty cycle is then achieved by application of transistor–transistor logic (TTL) square-wave signals to the laser controller by an arbitrary function generator (Tektronix, model AFG 3022B).

Measurement of the acoustic reflection–suppression efficiency of THORS barriers produced following excitation of ambient water vapor with the high-powered CO laser was performed using the setup depicted in Fig. 1a. Generation of acoustic waves of different audible frequencies was performed by driving an earbud speaker (JLabs, model J6M) with a function generator emitting a constant 3V amplitude, sinusoidal signal that can be varied in frequency from 2 to 20 kHz. The earbud speaker was placed several inches (greater than
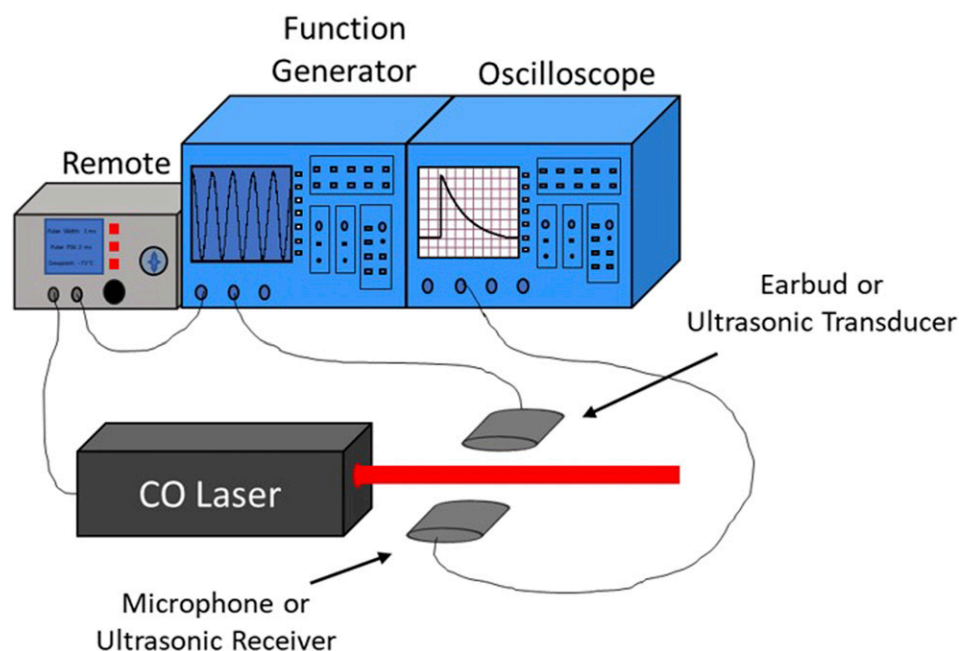
Figure 1. Experimental setup for measuring the suppression of acoustic/ultrasonic pulses incident on a THORS barrier. The output source (i.e., earbud for acoustic measurements or T/R transducer for ultrasonic measurements) and the acoustic/ultrasonic collector (i.e., microphone for acoustic measurements or ultrasonic transducer in RO mode for ultrasonic measurements) face each other on opposites sides of the barrier, both orthogonal to the direction of the laser beam.

one acoustic wavelength) from the CO laser beam.[13] On the opposite side of the laser beam, facing the earbud, a 2.54 mm nominal diameter, hearing aid microphone (Knowles, model FG-23629-P16) was placed 5 mm from the beam for acoustic detection and measurement of transmitted acoustic waves. The output of the microphone was recorded using a 500 MHz digital oscilloscope (LeCroy, Waverunner LT342). The signal from the function generator was used to synchronize the CO laser with the output of the acoustic wave to ensure the laser was present as the acoustic wave passed through the air where the THORS barrier should be present.

Results and Discussion

Quantification of the acoustic reflection–suppression efficiency of these THORS barriers generated in ambient air was performed by firing the CO laser at an optical modulation frequency of 100 kHz, with a 50% duty cycle, and measuring the amplitude of the acoustic wave striking the microphone in the absence (left side of Fig. 2a) or in the presence (right side of Fig. 2a) of the laser beam. Measurements in the absence of the THORS barrier were performed with the laser shutter closed. Measurements in the presence of the THORS barriers were performed with the laser shutter open. Signals for both "in the absence of THORS" and "in the presence of the THORS" barriers were each averaged over 100 different measurements. To quantify the efficiency of the THORS barriers at reflecting the incident sound wave, the difference in

acoustic amplitude between the signals with the laser shutter open and the shutter closed was divided by the amplitude of the signal when the laser shutter was closed and then multiplied by 100 to obtain a percentage. Figure 2a shows the amplitude of a typical acoustic wave (11.6 kHz in this case) measured by the microphone in the absence (left) and presence (right) of a THORS barrier. Similar measurements were made at various frequencies across the audible acoustic range (3–15 kHz; the optimal operating range of the microphone), revealing a relatively constant reflection–suppression efficiency independent of the incident acoustic frequency, as previously observed from ethanol-based THORS studies.[12] However, unlike previous measurements with ethanol saturated air following CO_2 laser based excitation, the suppression efficiency of the THORS barriers generated using the high-powered CO laser and ambient water vapor as the absorber was found to be 51 ± 5% across the audible range, a twofold increase over the previous maximum observed in ethanol-based measurements. The THORS acoustic suppression efficiency error bars represent the standard deviation of three replicate acquisitions.

To determine the efficacy and efficiency of THORS barriers for the reflection–suppression of acoustic waves outside of the audible frequency range, several discreet ultrasonic frequencies were also studied. Ultrasonic frequencies of 120, 200, and 300 kHz were employed due to the relatively minimal dampening of these frequencies in air and the readily available air coupled ultrasonic transducers and receivers at these
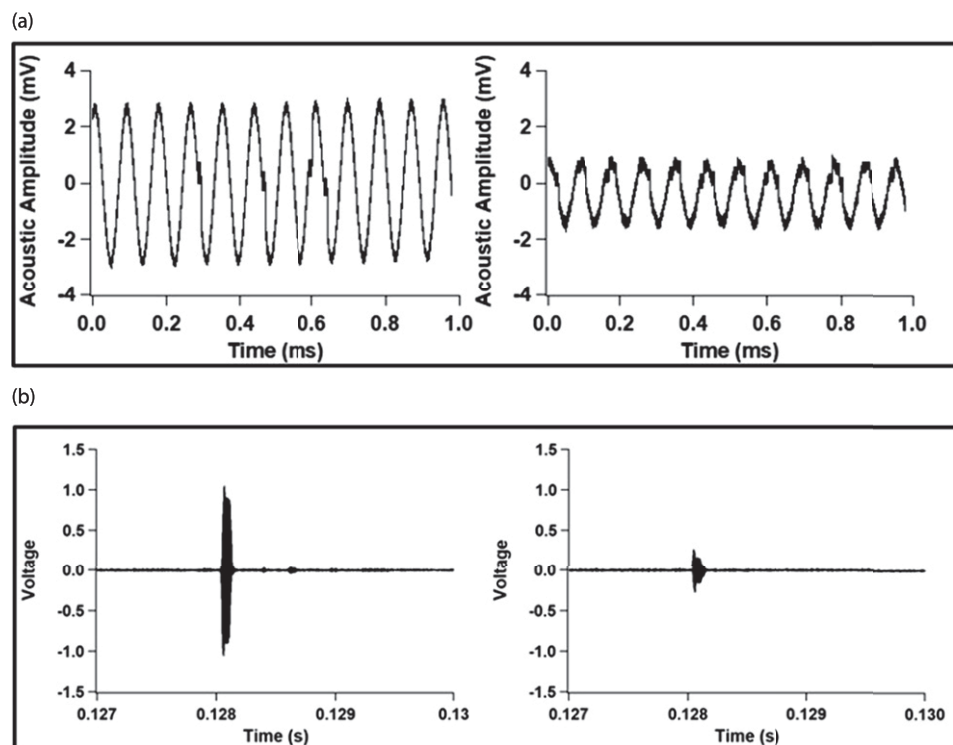
(a)

(b)

Figure 2. Oscilloscope traces of suppression measurements performed using the experimental arrangement described in Fig. 1 of (a) a 3 kHz acoustic wave measured by the microphone in the absence (left) and presence (right) of a THORS barrier and (b) a 300 kHz ultrasonic pulse measured by the RO transducer in the absence (left) and presence (right) of a THORS barrier.

frequencies. Like the audible acoustic suppression measurements (Fig. 1), an ultrasonic transducer (Airman, model AT 300b CH) was placed one inch from the CO laser beam path and an ultrasonic transducer of corresponding response frequency (Airman; Model AT 300b CH) was placed on the opposite side of the THORS barrier. Each of the transducers (emitter and receiver) were coupled to separate transceiver modules (Airmar, T1 Development Kit) to power and operate them to prevent any electronic artifacts from occurring between them. The emitting transducer was then operated in transmit/receive (T/R) mode, emitting an ultrasonic pulse wave at a repetition rate of 10 Hz and synchronized with the CO laser firing through the function generator to ensure measurements were taken midway through the laser pulse. The receiving transducer was operated in receive-only (RO) mode, to observe the amplitude of the ultrasonic wave transmitted across the THORS barrier. The outputs of both transducer transceiver modules were coupled to a 500 MHz oscilloscope for pulse wave amplitude measurements. The amplitude of the ultrasonic pulse transmitted across the THORS barrier was then measured by taking the peak-to-peak value of the receiving transducer's signal and averaged over 100 measurements.

Figure 2b shows the effect of the THORS barrier on the transmission of a 300 kHz ultrasonic signal, with the signal on the left corresponding to the amplitude of the transmitted wave in the absence of a THORS barrier (i.e., laser shuttered) and the signal on the right side showing the same 300 kHz signal amplitude transmitted across the THORS barrier (i.e., laser shutter open). The oscilloscope traces in Fig. 2b were taken with the laser firing at an optical modulation frequency of 3 kHz, at a 50% duty cycle. From these measurements, it was found that not only do THORS barriers provide reflection–suppression of ultrasonic frequencies as well as audible frequencies, but the suppression efficiency for these 300 kHz ultrasonic waves was found to be approximately 70 ± 3%. Similarly, when ultrasonic emitter/transducer pairs operating at 200 kHz (Airmar; Model AT 200 CH) and 120 kHz (Airmar; Model AT 120 CH) were evaluated, THORS suppression efficiencies of 68 ± 3% and 71 ± 4%, respectively, were measured, demonstrating a relatively constant THORS reflection–suppression efficiency across air transmittable ultrasonic frequencies. The THORS ultrasonic suppression efficiency error bars represent a single standard deviation of three replicate acquisitions at each ultrasonic frequency.

Temporal Dynamics of Thermally Induced Optical Reflection of SoundBarriers

To understand the temporal dynamics associated with the formation and decay of these THORS barriers generated in ambient air, temporally resolved suppression studies were
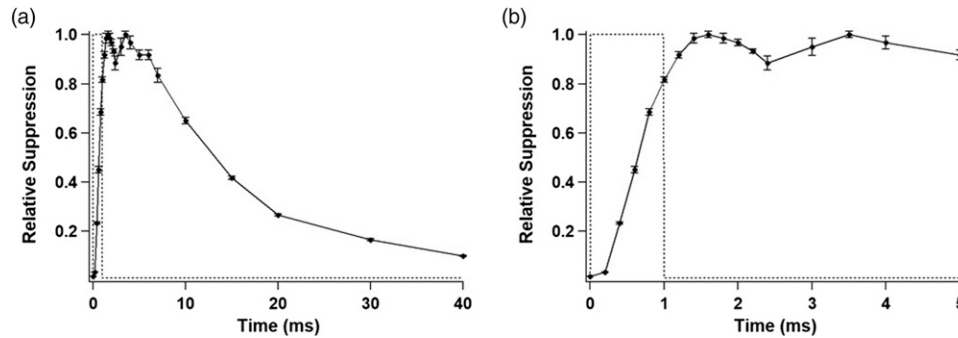
Figure 3. (a) The relative suppression efficiency of a 300 kHz ultrasonic signal incrementally delayed in time with respect to the start of a 1 ms duration laser pulse (shown by dotted square wave signal). Error bars represent one standard deviation of three replicate measurements at each data point. (b) Inset of the first 5 ms of panel a, revealing the rapid rise in the THORS barrier formation.

performed. In these studies, the suppression efficiency of 300 kHz ultrasonic signals was systematically measured as the ultrasonic pulse from the transducer was incrementally delayed in time with respect to the presence of a single CO laser excitation pulse. To synchronize the phase of the ultrasonic pulse with the laser used to generate the THORS barrier, the output signal of the 300 kHz emitter was coupled to the function generator controlling the firing of the laser. The emitter was set to provide 300 kHz ultrasonic pulses at a repetition rate of 10 Hz. Each emitter pulse triggered a laser pulse, by coupling the output of the function generator to the laser remote external TTL input, resulting in laser emission, equal in duration to the TTL pulse. The timing sequence for these experiments was observed on the oscilloscope, where the TTL output from laser remote was coupled to channel 1 and the receiving ultrasonic transducer signal was coupled to channel 2. The oscilloscope was set to trigger on the positive slope of the laser pulse TTL signal. The TTL output to the laser was initially delayed by 100 ms from the emitter pulse, where the positive slope of the laser TTL signal overlapped the subsequent ultrasonic pulse. By reducing the delay time between the emitted ultrasonic pulse and laser pulse, the receiving transducer signal effectively moves forward in time with respect to the CO laser output. The electronic delay between the time laser trigger pulse and laser emission is approximately 20 µs, with a jitter of less than 10 µs. To ensure all temporal measurements were statistically different, increments in the delay between the laser pulse and ultrasonic pulse were a minimum of 200 µs. By shifting the phase delay between the ultrasonic pulse and the laser trigger pulse, it is possible to alter the timing between the presence of the laser and the ultrasonic signal, with 10 µs resolution or better, and allow for ultrasonic suppression to be measured over the entire time course of the THORS barrier (prior to laser pulse being emitted through the firing of the subsequent laser pulse). By monitoring the reflection–suppression efficiency of the 300 kHz ultrasonic signal, it is possible to probe the THORS barrier with high enough temporal resolution to observe its formation and decay.

The results from this study can be seen in Fig. 3, in which the relative suppression efficiency of the THORS barrier as a function of time, relative to the beginning of a 1 ms CO laser pulse, is plotted. The timing of the 1 ms CO laser pulse (250 W) is shown by the dotted square wave signal while the individual data points (and associated trend lines) represent relative suppression efficiency of the transmitted ultrasonic wave. Each data point is the averaged value of three suppression measurements acquired by averaging the ultrasonic signal over 100 sweeps on the oscilloscope. The error bars in Figures 3a and b represent one standard deviation of the three averaged measurements. Measurements between zero and 2.4 ms were acquired in 200 µs time increments, where the incremental step size increased to 0.5 ms, 1 ms, 3 ms, 5 ms, and 10 ms between 3 ms, 4 ms, 7 ms, 10 ms, and 20 ms, respectively. The change in delay increments was chosen, to reduce the experimental acquisition time, while still providing valuable insights into the formation and decay dynamics of the barrier. From this plot (Fig. 3b shows an expansion of the first five ms of the plot in Fig. 3a), a statistically measurable rise in acoustic suppression occurs within 200 µs of initiation of the laser pulse. Although this is statistically measurable, with a relative suppression change of approximately 0.016, a significant increase is not observed until 400 µs where the relative suppression change is approximately 0.2. Suppression then rapidly increases, at a nearly constant rate (3.94%/ms) until it reaches a maximum in suppression at approximately 1.4 ms after the laser pulse begins (400 ms after the laser has finished firing), demonstrating the rapid generation of the compressibility barrier between the excited volume and the surrounding air. Once the laser is off, the maximum reflection–suppression efficiency of the THORS barrier is sustained for an additional 5–6 ms. After this time, the suppression efficiency of the THORS barrier decays rapidly, consistent with molecular diffusion rates of atmospheric gases (i.e., repopulation of the depleted volume).[20] Approximately 40–50 ms following excitation, no measurable suppression (i.e., THORS barrier) exists until the next excitation pulse.
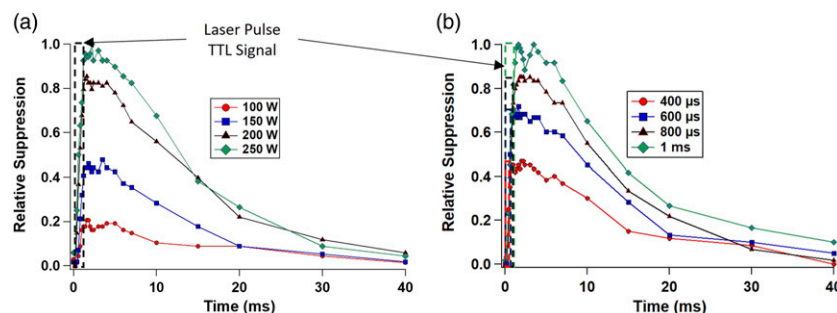
Figure 4. (a) Time dependent relative acoustic suppression efficiencies of THORS barriers generated following a 1 ms duration laser pulse of different powers. Dotted square wave represents the pulse duration of the 1 ms excitation laser. (b) Time dependent acoustic suppression efficiency of THORS barriers generated with different pulse duration excitation pulses, including 400 μs, 600 μs, 800 μs, and 1 μs. Each data point in these plots corresponds to three averaged suppression measurements. Error bars represent one standard deviation but are not visible on the graph as they are smaller than the data points.

Effect of Laser Power–Energy Deposited on Thermally Induced Optical Reflection of Sound Temporal Dynamics

Due to the photothermal nature of the THORS phenomenon, the effect of laser power (i.e., energy deposited) on both the relative magnitude of the THORS reflection–suppression efficiency as well as the temporal dynamics of the barrier generation and decay were investigated. In these studies, laser powers of 250 W (100%), 200 W (80%), 150 W (60%), and 100 W (40%) were used for excitation of the ambient water vapor via one ms excitation pulses from the CO laser. The results of these power studies are shown in Fig. 4a. As expected from photothermal phenomena and observed previously with THORS studies in ethanol vapor,[13] the efficiency of the THORS barrier increases with increasing excitation power in a nonlinear fashion, with a rapid increase in reflection–suppression efficiency occurring after a minimal excitation power is employed and then rapidly increasing and leveling off at higher excitation powers. In these studies, the 250 W laser pulse results in the greatest ultrasonic suppression maximum (normalized to one) with each subsequent lower laser power excitation pulse providing significantly less; 200 W (80% laser power) providing 0.84 ± 0.04, 150 W (60% laser power) proving 0.57 ± 0.02, and 100 W (40% laser power) providing 0.225 ± 0.002 suppression. Despite different maximum suppression amplitudes, a rapid increase in suppression efficiency occurs within the first 200 ms of the start of the excitation pulse, with the suppression maximum being achieved approximately 400 ms after the laser pulse ends and continuing at this maximum suppression efficiency for 5–6 ms. Furthermore, the lower power excitation pulses (i.e., 150 W and 100 W), exhibit a slightly diminished rate of suppression increase during the excitation pulse, consistent with what might be expected for the deposition of energy into the system, with the lower laser powers providing less energy per time and thereby slightly decreasing the rate at which the

THORS barrier achieves its maximum capability. Furthermore, as observed for the previous measurements, within tens of milliseconds (i.e., 40–50 ms) after excitation from the one ms pulse, the THORS barrier completely decays, resulting in a temporally transient barrier for acoustic manipulation that can be regenerated with each subsequent excitation pulse.

Because photothermal events are dependent upon both the total energy applied to the system (i.e., total energy absorbed by the water vapor) as well as the rate at which the absorption occurs, the effect of laser pulse duration on the overall THORS suppression was also studied in addition to varying the power with a constant 1 ms laser pulse. With the CO laser operating at its maximum output power (250 W) for all pulse durations, THORS suppression/reflection measurements were obtained for laser pulse durations of 1 ms, 800 μs, 600 μs and 400 μs. These pulse durations result in the same amount of total energy being delivered to the air as in the power studies (i.e., 800 μs being 80%, 600 μs being 60%, and 400 μs being 40%) but delivered at the same rate as the maximum power pulse. The results of this study are shown in Fig. 4b. Each data point in Figs. 4a and 4b represent the average value of three suppression measurements acquired by averaging the ultrasonic signal over 100 sweeps on the oscilloscope for each measurement. Error bars are included in the graph as the one standard deviation of these values but are too small to be visible on the graph. As previously observed in the laser power studies, the greater the total amount of energy deposited in the air, the greater the THORS suppression efficiency. Specifically, the 800 μs pulse provided 0.82 ± 0.08 relative suppression, the 600 μs pulse provided 0.70 ± 0.03 relative suppression, and the 400 μs pulse provided 0.438 ± 0.004 relative suppression. From these results, the two shortest pulse durations resulted in greater overall maximum suppression efficiencies compared to the power studies, which is attributed to the increase in the rate at which the energy was deposited in the air. This can be seen by the same rapid rate of suppression efficiency increase for all pulse
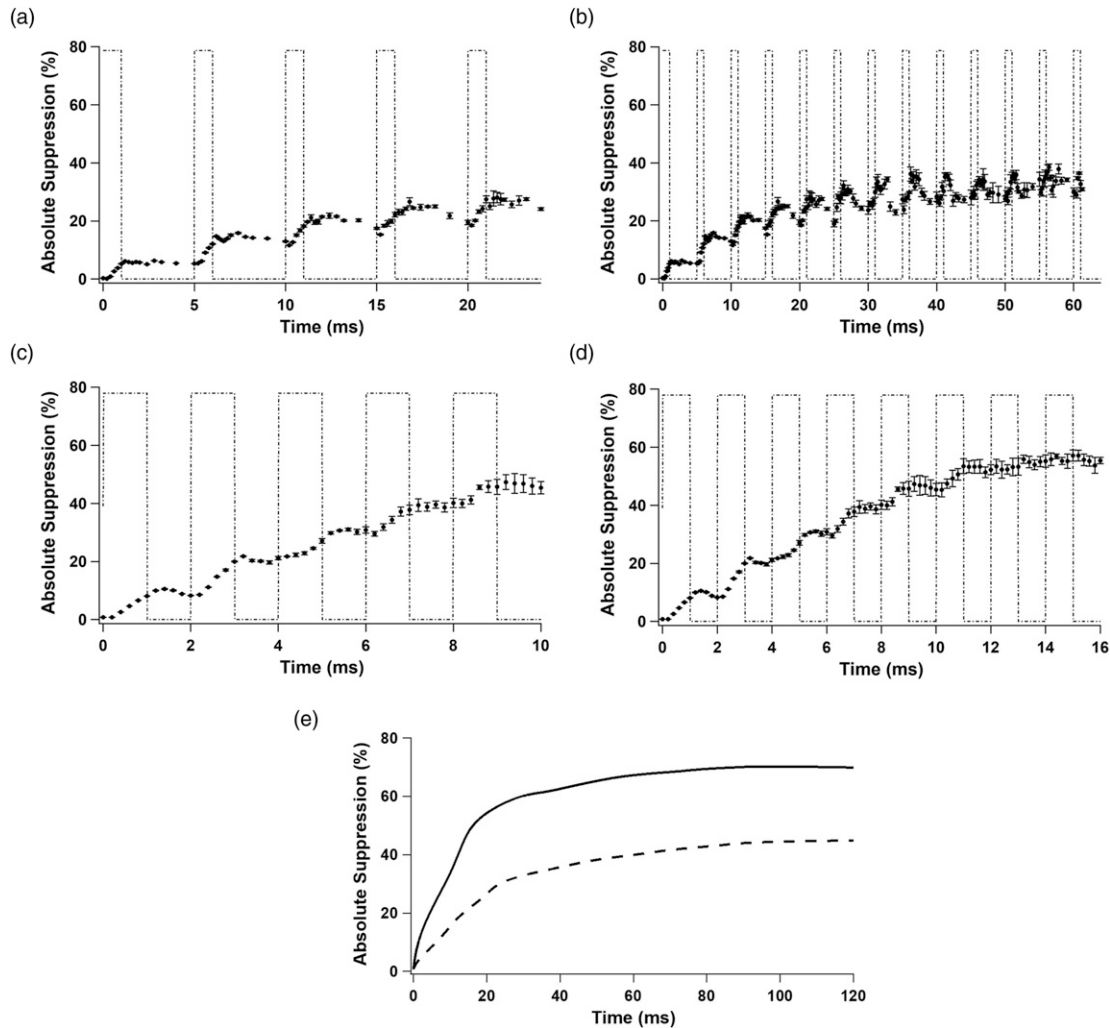
Figure 5. (a) THORS suppression efficiency measured as a function of time with 1 ms duration laser pulses (square wave) fired every 5 ms. (b) Extended data of Fig. 5a over 60 ms. (c) THORS suppression efficiency measured as a function of time with 1 ms duration laser pulses (square wave) fired every 2 ms. (d) Extended data of Fig. 5c over 16 ms. (e) The suppression efficiency for laser off times of 1 ms (dashed trend line) and 4 ms (solid trend line) measured over the course of 120 ms. Error bars for figures (a–d) represent one standard deviation of three replicate measurements at each data point.

durations during the barrier formation, which is to be expected since the power of the laser was constant over the excitation time.

Temporal Dynamics of Multi-Excitation

Unlike the maximum acoustic suppression efficiencies observed in Fig. 1 (i.e., 70%), which were performed after repetitively firing the laser in the air, the maximum suppression efficiencies observed for the temporally resolved studies following single excitation pulses of the CO laser (Figs. 2 and 3), resulted in absolute suppression efficiencies of only 8.5 ± 0.2% of the incident signal (for 250 W, 1 ms duration pulses) corresponding to a significant decrease in the efficacy of the THORS barriers as observed in Fig. 1. To understand the

reason for this significant decrease in efficacy of the THORS barriers following a single excitation pulse, as well as to understand the effect that delivering subsequent excitation pulses prior to complete decay of the THORS barrier has on the total suppression, a series of acoustic suppression studies were performed with multiple excitation pulses delivered following different delay times.

Since THORS barriers generated by individual, 1 ms excitation pulses were found to exhibit a continuous maximum in transmission suppression efficiency for approximately 5–6 ms after excitation, time resolved suppression studies were performed with the CO laser firing one ms duration excitation pulses followed by a 4 ms delay prior to the next subsequent pulse. The results from these studies are shown in Fig. 5a (for the first five excitation pulses), with measurement

of the suppression efficiency of the incident 300 kHz ultrasonic probe pulses occurring at 200 ms increments. By monitoring the suppression efficiency at 200 ms increments, it is possible to observe the changes to the THORS barrier both during each individual excitation pulse (denoted by the positive square wave) as well as in between each pulse (denoted by the negative portion of the square wave). In these studies, each suppression efficiency measurement corresponds to the average of three measurements with the error bars corresponding to a single standard deviation. As can be seen from Fig. 5a, during the first excitation pulse, the relative THORS suppression efficiency increases to an absolute value of 6.12 ± 0.07% and remains constant at this value during the subsequent 4 ms, as previously observed in the single pulse dynamics studies. Upon the arrival of the second excitation pulse the suppression efficiency increases to 15.8 ± 0.3% resulting in a total suppression that is the summative result of each individual excitation event. However, following the second excitation pulse, the suppression efficiency is slightly decreased to 11.6 ± 0.1% prior to the arrival of the third excitation pulse. Once again, as the third excitation pulse is present, the suppression efficiency increases again to 21.8 ± 0.9% with a subsequent decrease to 15.3 ± 0.2% in the following 4 ms. This repeated increase in suppression efficiency and subsequent increasing rate of decline in the magnitude of the acoustic suppression efficiency after the laser is no longer present continues until all gains in suppression with each subsequent excitation pulse are negated by the rapid decline in suppression between pulses, resulting in the overall suppression efficiency leveling off after a number of laser pulses. Figure 5b shows this same data over a time of 60 ms (corresponding to 13 excitation pulses), revealing an absolute maximum THORS barrier suppression efficiency of 38 ± 1% is achieved after approximately 50–60 ms (11–12 laser pulses) with minimal increases after this point if the laser continues to fire at the same frequency. In fact, suppression efficiency measurements taken 3 h later (data not shown) reveal a maximum absolute suppression efficiency of 45 ± 2%, demonstrating the ability to maintain a constant THORS barrier with modulated excitation if the duration between pulses remains under 5 ms. Furthermore, this study demonstrates that it is possible to control the magnitude of the acoustic manipulation (reflection or suppression) obtained by THORS barriers, between zero and the maximum, simply by altering the number of sequential laser pulses employed.

With the 4 ms delay in between excitation pulses allowing for rapid declines in suppression efficiency to occur in the THORS barriers generated by repeated laser pulses, similar acoustic suppression studies were performed with increasingly shorter off times between excitation pulses, ranging from 200 μs between subsequent 1 ms pulses to the four ms delay described above. Figure 5c shows the results obtained from repeated 1 ms excitation pulses separated by a 1 ms off time. Like the results from Fig. 5a, with each excitation pulse, the acoustic suppression efficiency of the barrier increased by 9 ± 2% for the first four pulses. However, by decreasing the time between subsequent excitation events to 1 ms, no statistically significant decrease in suppression efficiency was observed between pulses. However, after the sixth excitation pulse (as shown in Fig. 5d), when the suppression efficiency reached a value of 53 ± 2%, only small diminishing increases (<1%) in suppression efficiency are observed with each subsequent excitation event, again resulting in a leveling off effect for the maximum suppression level. At the same time, the increase in suppression efficiency with each subsequent pulse begins to decrease, the variability in individual suppression measurements increases and levels off as well, which is what would be expected for a photothermal phenomenon achieving local thermal equilibrium (i.e., no further increase in localized heat occurring). This ultimately results in a maximum achievable THORS barrier efficiency of 72 ± 5% exists (for an individual THORS barrier) by exciting the specific concentration of water vapor in the air. By shortening the time between subsequent excitation events from a 4 to 1 ms delay shown in Figs. 4a and 4c and removing the decrease in suppression efficiency that occurred between excitation events, it was possible to increase the maximum THORS barrier acoustic suppression from 45 ± 2% to 72 ± 5% (Fig. 5e). In addition, by shortening the off time between subsequent laser pulses, the time required to achieve maximum suppression was also decreased. In both cases, the maximum suppression efficiency achieved was able to be maintained indefinitely over the 3 h monitored. These same trends of increasing overall suppression efficiency and decreasing the time necessary to achieve maximum suppression with decreasing off times was observed for all off times evaluated, except for off times of less than 1 ms between the laser pulses (i.e., 200 ms, 400 ms, 600 ms, 800 ms). These off-time durations between pulses all showed statistically equal maximum suppression efficiencies and timing to those of the 1 ms off times.

In addition to evaluating the effect that different off times between multiple excitation events has on the overall efficiency of the THORS barriers, characterization of the effect that different duration excitation pulses have on THORS reflection–suppression efficiency for barriers generated with repetitive excitation was also studied. To provide a consistent off time for these studies, one ms between subsequent pulses was chosen. One millisecond off times were chosen because: (i) 1 ms after excitation, THORS suppression efficiencies remain at their maximum (for all duration laser pulses studies via isolated excitation events (Fig. 3), and (ii) during multiple excitation pulse studies, no decrease in THORS suppression efficiency between pulses could be observed for 1 ms off times (as seen in Fig. 5), thereby allowing the effect of variable excitation durations to be studied independent of the THORS barrier degradation effects between subsequent pulses.

Results from this study are shown in Fig. 6. As can be seen from the plots for one ms (solid circles), 400 μs (solid triangles) and 200 μs (solid squares) duration excitation pulses, as expected, the shorter the duration of the excitation pulse,
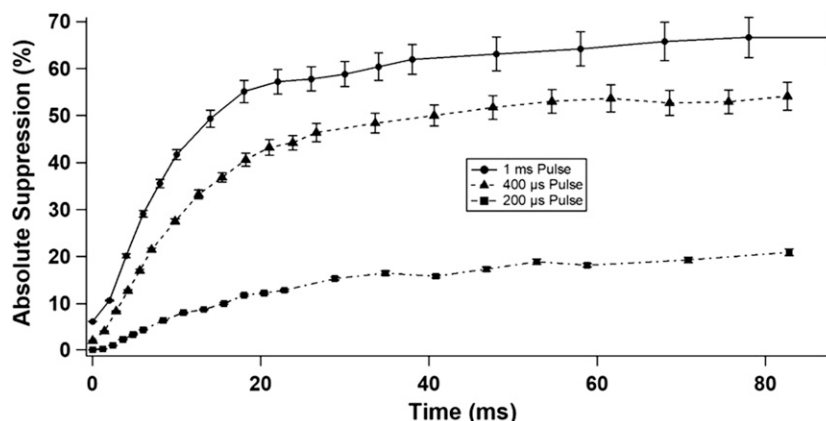
Figure 6. Measured THORS suppression efficiencies over a span of 80 ms, for THORS barriers generated by excitation pulses of 200 μs duration (solid squares), 400 μs duration (solid triangles) and 1 ms duration (solid circles); each with 1 ms delay between subsequent excitation pulses. Error bars represent one standard deviation of three replicate measurements at each data point.

the lower the overall suppression efficiency of the THORS barrier generated, due to the lower energy deposited into the air. In addition, the rate (i.e., number of excitation pulses) at which the maximum THORS suppression efficiency is achieved also varies with pulse duration, with the 1 ms duration excitation pulses providing a maximum suppression after 40 ms and the 400 μs duration pulses achieving maximum sustained suppression after 50 ms. In the case of the 200 μs duration laser pulses, a slight increase in THORS suppression continues even after 60 ms from the initial pulse, in each case increasing by 2 ± 1%, with maximum suppression of 22.6 ± 0.7% only being achieved after 83 ms (i.e., 69 excitation pulses). Therefore, by controlling the laser pulse duration, it is possible to easily control both the absolute magnitude of THORS acoustic reflection–suppression as well as the rate of increase; with longer duration pulses resulting in rapid and maximum suppression and shorter duration pulses proving a gradual and reduced reflection–suppression efficiency by THORS barriers generated by multiple sequential pulses.

Three Regimes for Thermally Induced Optical Reflection of Sound Barrier Excitation

Based on these temporal dynamics studies as well as previous continuous wave (CW) excitation studies and CW studies with the CO laser (results not shown), THORS barrier generation falls into one of three distinct operational regimes depending on the modulation frequency of the excitation source. In the first regime, the optical modulation frequency of the excitation source is slower than 50–60 ms, resulting in each excitation pulse generating an isolated barrier with minimal overall reflection–suppression efficiency (e.g., approximately 10% or less) that dynamically changes over a period of tens of milliseconds (50–60 ms). However, as the modulation frequency of the excitation source increases

between 10 Hz–200 kHz (the maximum operational frequency of the CO laser), a different additive phenomenon is observed, with the generation of a continuously present THORS barrier, despite being excited by a modulated source. If the optical modulation frequency is high enough to deliver subsequent excitation pulses prior to the complete decay of the THORS barrier (within approximately 50–60 ms; depending on the magnitude of the excitation), the magnitude of the reflection–suppression efficiency increases with each additional excitation pulse until a maximum suppression is achieved that can be as great as 70% or more depending on the ambient humidity. Finally, as observed for both previous CW excited THORS barriers in ethanol vapor,[13] as well as following quasi-CW excitation of water vapor with the CO laser, no significant acoustic reflection–suppression is observable for any extended period of time. While the initial excitation event can generate a weak transient THORS barrier, similar to an isolated single shot based THORS barrier, the constant absorption of the laser continues to excite the air, generating a thermal gradient into the air surrounding the THORS barrier. This thermal gradient then allows the acoustic wave to be transmitted with minimal reflection–suppression through the optically excited region, analogous to anti-reflection coatings using a gradient refractive index,[21] resulting in the complete loss of all THORS reflection–suppression.

Conclusion

This paper has demonstrated for the first time the ability to generate THORS barriers in ambient air through the excitation of water vapor with a CO laser. In addition, these THORS barriers have been demonstrated to be capable of manipulating both audible acoustic as well as ultrasonic waves with a high degree of efficiency (greater than 70%). Furthermore, by altering the optical modulation frequency of the

excitation source employed, it is possible to generate either transient THORS barriers with varying acoustic reflection abilities over a period of tens of milliseconds, or constantly present THORS barrier capable of continuously reflecting greater than 70% of the incident acoustic or ultrasonic wave incident on the barrier. This ability to generate THORS barriers in ambient air that are capable of optically manipulating audible as well as ultrasonic waves in a continuous fashion open the possibility of numerous real-world applications of THORS such as acoustic stealth technologies, secure communications, standoff photoacoustic spectroscopy, and acoustic steering.

Future studies will focus on charactering the spatial geometry and dynamics of the THORS barriers through time resolved chemical imaging of the various molecular species present (i.e., N_2 and water vapor) to understand the spatial dimensions of the barriers and the relative density differences between the excited volume and the surrounding air. In addition, with the temporal dynamics characterized, application of optimized THORS barriers for standoff photoacoustic sensing and enhanced resolution photoacoustic imaging will also be explored.

Declaration of Conflicting Interests

The author(s) declared no potential conflicts of interest with respect to the research, authorship, and/or publication of this article.

ORCID iD

Brian M. Cullum ⓘ https://orcid.org/0000-0002-5250-8290

References

1. F.J. Fahy. "Impedance". Foundations of Engineering Acoustics. London, UK: Academic Press, 2000. Vol. 1. Chap. 4, Pp. 48-71.
2. M. Moser. "Noise Barriers". Engineering Acoustics. New York: Springer, 2014. Vol. 1. Chap. 10, Pp. 311-343.
3. A.C. Tam. "Applications of Photoacoustic Sensing Techniques". Rev. Mod. Phys. 1986. 58(2): 381-426.
4. M. Xu, L.V. Wang. "Photoacoustic Imaging in Biomedicine". Rev. Sci. Instrum. 2006. 77(4): 41101041124.
5. V. Romero-García, N. Lamothe, G. Theocharis, O. Richoux, L. García-Raffi. "Stealth Acoustic Materials". Phys. Rev. Appl. 2019. 11(5): 054076.
6. G. Wen, Y. Lu, Z. Zhang, C. Ma, et.al. "Line Spectra Reduction and Vibration Isolation via Modified Projective Synchronization for Acoustic Stealth of Submarines". J. Sound Vib. 2009. 324(3-5): 954-961.
7. D. Volpano, C. Irvine, G. Smith. "A Sound Type System for Secure Flow Analysis". J. Comput. Secur. 1996. 4(2-3): 167-187.
8. S. Vaudenay. "Secure Communications Over Insecure Channels Based on Short Authenticated Strings". Lect. Notes. Comput. Sci. 2005. 3621: 309-326.
9. R.S. Little. "Acoustic Properties of Parabolic Reflectors". J. Acoust. Soc. Am. 1966. 40(4): 919-920.
10. D. Zhao, X. Li. "A Review of Acoustic Dampers Applied to Combustion Chambers in Aerospace Industry". Prog. Aero. Sci. 2015. 74: 114-130.
11. M. Stojanovic, J.A.J.G. CatipovicProakis. "Phase-Coherent Digital Communications for Underwater Acoustic Channels". IEEE J. Ocean. Eng. 1994. 19(1): 100-111.
12. D.S. Kazal, A. Ngo, E.L. Holthoff, B.M. Cullum. "Acoustic Steering Using Thermally Induced Optical Reflection of Sound (THORS)". Appl. Spectrosc. 2021. 75(10): 1320-1326.
13. B.M. Cullum, E.L. Holthoff, P.M. Pellegrino. "Optical Reflection and Waveguiding of Sound by Photo-Thermally Induced Barriers". Opt. Express. 2017. 25(19): 22738-22749.
14. L.E. Kinsler, A.R. Frey, A.B. Coppens, J.V. Sanders. "Absorption and Attenuation of Sound". In: L.E. Kinsler, editor. Fundamentals of Acoustics. Hoboken, NJ: John Wiley and Sons, 2000. Chap. 8, Pp. 210-238.
15. P.M. Morse, K.U. Ingard. Theoretical Acoustics. Princeton: Princeton University Press, 1986. Pp. 524-567.
16. C.W. Van Neste, L.R. Senesac, T. Thundat. "Standoff Photoacoustic Spectroscopy". Appl. Phys. Lett. 2008. 92(23): 234102.
17. L.S. Marcus, E.L. Holthoff, P.M. Pellegrino. "Standoff Photoacoustic Spectroscopy of Explosives". Appl. Spectrosc. 2017. 71(5): 833-838.
18. X. Chen, L. Cheng, D. Guo, Y. Kostov, F.-S. Choa. "Quantum Cascade Laser Based Standoff Photoacoustic Chemical Detection". Opt. Express. 2011. 19(21): 20251-20257.
19. F. Dalby, H. Nielsen. "Infrared Spectrum of Water Vapor. Part I: The 6.26 μm Region". J. Chem. Phys. 1956. 25(5): 934-940.
20. W.G. Vincenti, C.H. Kruger. Introduction to Physical Gas Dynamics. Ann Arbor, MI: Kreiger, 1975. Pp. 332-418.
21. I.M. Thomas. "High Laser Damage Threshold Porous Silica Antireflective Coating". Appl. Opt. 1986. 25(9): 1481-1483.